A miniature free-piston engine/compressor

Authors: Lei Tian[1], David B Kittelson[1], William K Durfee[1]*

Affiliations:

[1]Department of Mechanical Engineering, University of Minnesota, USA.

*Corresponding author. Email: wkdurfee@umn.edu

Abstract

Portable powered devices such as construction tools and orthotics require a power supply that is light and compact. Hydrocarbon fuel has exceptionally high energy density compared to batteries but must be converted to mechanical power to be useful. We designed, constructed and evaluated a tiny internal combustion air compressor that uses a free-piston configuration combined with homogeneous charge compression ignition. The device compressed air in a small tank to 6.5 bar with an overall fuel to cold compressed air efficiency of 0.6%. The engine was self-regulating with the compression ratio automatically adjusting for variations in load and speed. Unlike a traditional crankshaft engine, the piston is not constrained and expansion is rapid so that combustion continues during expansion lowering efficiency. Switching from glow plug to true homogeneous charge compression ignition, which has fast kinetics will improve system efficiency as will better sealing to prevent blow-by leakage. Our mathematical model was able to predict the essential experimental results from the prototype engine.

Keywords

HCCI, Engine-compressor, Portable power supply, engine modeling, combustion modeling

1. Background

Portable tools and wearable assistance machines require a compact, lightweight power supply. Competing technologies include batteries, fuel cells and compressed gas. However, few energy sources have the enormous energy density of hydrocarbon fuels. For example, the energy density of gasoline is about 47 MJ/kg compared to 1.8 MJ/kg for lithium polymer batteries. Thus there is motivation to develop compact power supplies that use hydrocarbon fuel as the source and produce an output that can be directly used to drive small machines. One particularly useful power output is compressed air as it is clean, has high energy density and can drive light weight air cylinders and air motors. While mains, battery and internal combustion engine powered air compressors are standard, they are either tethered or too large and too heavy for wearing. Our approach to this problem was to use homogeneous charge compression ignition (HCCI) driving a free-piston engine and combined with a compressor to produce what we believe to be the smallest internal combustion air compressor.

Despite the advantages of micro-combustion for a power supply, significant technical obstacles present barriers to practical use including combustion control, quenching, exhaust gas

scavenging, thermal management, friction, sealing, starting and fabrication of small, precise parts that operate at high temperatures. The significance of these barriers increases as the engine size decreases because of area-to-volume and circumference-to-area scaling.

A free-piston internal combustion engine has no crankshaft. Without the kinematic constraint of a crankshaft, the movement of the piston is driven down by pressure in the combustion chamber and up by a rebound spring. Compared to a crankshaft engine, the free-piston configuration is compact with fewer moving parts and no side thrust between piston and cylinder wall. Unlike a crankshaft engine, the piston motion must be constrained for compression ratio, ignition timing and scavenging [1]. Large free-piston engine air compressors are well known (e.g. Pescara [2], Junker [3] and Braun [4]) and there has been some work at small scales (e.g. the 100 W engine by Riofrio [5] and the 500 W engine by Aerodyne Research [6].) In large free piston engines, various control schemes are used to regulate piston motion, including controlling the rebound energy for controlling engine compression ratio [7] and engine frequency modulation [8]. In a miniature engine design, implementing sensors and actuators is challenging, therefore our engine was designed to run autonomously without any active control of engine speed, load, ignition timing, fuel-air mixture or piston position.

HCCI combustion mode where the fuel-air mixture is compressed until it auto-ignites [9] is appropriate for free-piston, micro-combustion engines. Combustion timing is a challenge in conventional crankshaft HCCI engines but adjusts naturally in a free-piston engine as the piston continues to compress the mixture until it auto-ignites. Ignition is nearly simultaneous within the combustion chamber so there is no propagating flame to quench against the relatively large surface area of a tiny engine. No spark plug or fuel injector is needed, which means tiny bore cylinders can be realized. Finally, HCCI combustion rate is determined by chemical kinetics rather than by flame propagation, which means a small engine can be run at exceptionally high cycle speeds to produce reasonable power. Aichlmayr, who proposed the concept of a tiny free-piston HCCI engine-compressor [10,11], experimentally demonstrated that HCCI can occur in a 3 mm bore cylinder [12], but did not create a working engine.

We designed a 12.5 mm bore, two-stroke, free-piston engine/compressor and built a prototype (Fig. 1). The device is 12 cm long and weighs 260 grams. The prototype uses glow plug ignition, which like HCCI has naturally adjusted timing, but makes the engine easier to start and lowers the required compression ratio.

Carburetor

Silencer

Engine piston

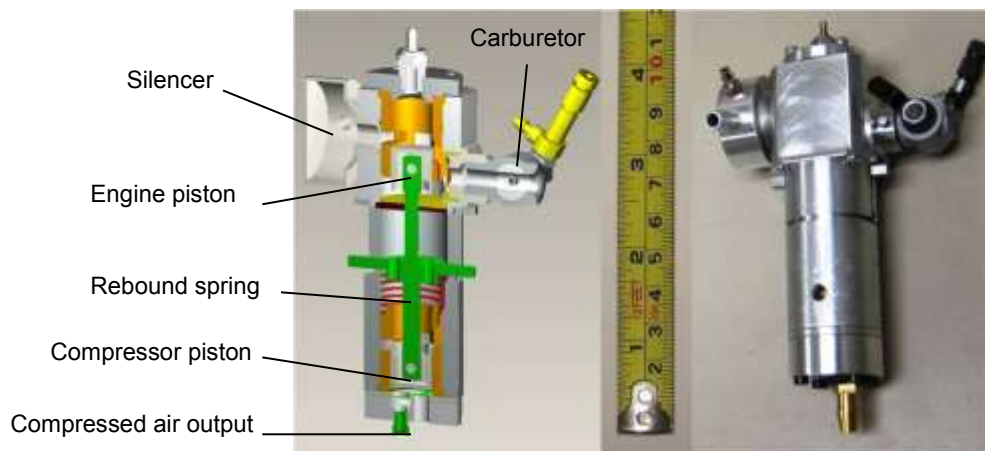Rebound spring

Compressor piston

Compressed air output

2

Fig. 1. Free-piston engine/compressor rendering and prototype. On the engine (upper) end, fuel air mixture induction results from the upward motion of the piston drawing the fresh mixture from the carburetor into the crankcase through a low mass reed intake check valve with Schnuerle type scavenging. Downward piston motion compresses the fresh mixture inside the crankcase, forcing it to flow around and up into the cylinder space above the piston ready for compression and combustion. On the compressor (lower) end, the reciprocating compressor piston draws in ambient air and outputs compressed air through inlet and outlet reed check valves. The downward motion of the piston is driven by the expanding combustion products inside the engine cylinder and the upward return motion is driven by the metal rebound spring and by residual compressed air below the compressor piston..

2. Engine model

2.1. Model overview

An overall mathematical model of the engine/compressor was developed based on a previous model of a 1.5 cc glow-ignition two-stroke engine [13] with important model components briefly described here. We experimentally tested components of the engine/compressor, including check valve response, blow-by leakage, friction, scavenging process and combustion process to provide parameters for the mathematical model. Because the prototype we built was similar in size to and used several components (e.g. the piston and cylinder liner) from a 1.5 cc, glow-ignition two stroke engine, some of the component parameter characterization was done by testing a two stroke engine (Hornet 09 R/C Engine, AP Engines).

2.2. Piston leakage

An essential characteristic to model in miniature engines is the blow-by leakage through the gap between engine piston and cylinder. This loss is unimportant in full scale engines but as engine size goes down, the gap width between piston and cylinder stays approximately the same as it is mostly determined by machining tolerances. Thus, blow-by leakage is more important in miniature engines since the leaked mass can be a large fraction of in-cylinder charge. An orifice flow model was used to calculate the flow rate through the piston-cylinder gap

$$\frac{dm}{dt} = C_d A_o P_{o1} \sqrt{\frac{2}{R_m T_{o1}}} \times \Psi$$

where dm/dt is the blow-by flow rate, A_o is the reference intake channel area, C_d is the flow coefficient, subscripts 1 and 2 indicate upstream and downstream properties and subscript o indicates stagnation parameters. The flow function ψ for subsonic flow and sonic flow is

$$\Psi_{sub-sonic} = \sqrt{\frac{\gamma}{\gamma - 1}\left[\left(\frac{p_2}{p_{o1}}\right)^{\frac{2}{\gamma}} - \left(\frac{p_2}{p_{o1}}\right)^{\frac{\gamma+1}{\gamma}}\right]}$$

$$\Psi_{sonic} = \left(\frac{2}{\gamma + 1}\right)^{\frac{1}{\gamma-1}} \sqrt{\frac{\gamma}{\gamma + 1}}$$

where γ is the ratio of specific heats. The gap width was assumed to be 20 μm as recommended by Sher [14].

The leakage model was validated by motoring a 1.47 cc 2-stroke engine (Hornet 09, AP Engines) without combustion. Figure 2 shows experimental results for peak pressure as a function of engine speed, along with the theoretical prediction that combines heat transfer and blow-by leakage. The data shows that both heat transfer and leakage decrease peak motoring pressure as engine speed decreases because the engine has more time to lose heat through heat transfer and more time to lose in-cylinder mass through leakage. The conclusion is that miniature engines should be run at high speed to avoid excessive blow-by leakage and heat loss to improve efficiency.
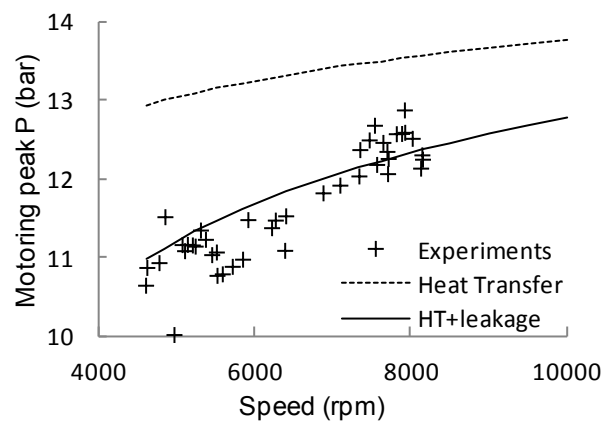

Fig. 2. Leakage model prediction of motoring peak pressure versus motoring speed, and comparison with experimental data from non-combustion engine motoring.

2.3. Piston friction

Friction has a bigger effect in miniature engines than in full scale engines because of the larger surface to volume ratio. In addition, miniature two-stroke model engine fuel contains up to 20% lubricating oil and friction related to the resulting thick layer of lubrication oil can be significant.

The friction level in an engine is typically described by the friction mean effective pressure (FMEP)

$$\text{FMEP} = \frac{\text{Friction work per cylinder per cycle}}{\text{Swept volume per cylinder}}$$

For a two-stroke engine Heywood and Sher [15] recommend modeling friction as a function of speed using a second-order polynomial

$$\text{FMEP} = a + b\left(\frac{N}{1000}\right) + c\left(\frac{N}{1000}\right)^2$$

where FMEP is in kPa and engine speed N is in rpm. In a free piston engine, however, friction should be modeled as a function of piston speed, thus the appropriate equation is

$$f = a + bv + cv^2$$

where f is friction in N, v is piston speed in m/s and a, b, and c are coefficients related to mechanical, hydrodynamic and aerodynamic friction respectively.

The experimental data from non-combustion motoring of the 1.5 cc 2-stroke engine were used to parameterize the friction model. Friction was estimated from the difference between indicated output power output and brake power and from this the mechanical efficiency was determined. Using a least-squares fitting process, a, b and c were determined to be 1.6, 0.5 and 0.04. Modeling and experimental results are shown in Fig. 3. The mechanical efficiency of this engine was around 70% at low speed and dropped rapidly at speeds higher than 10000 cycles per minute.
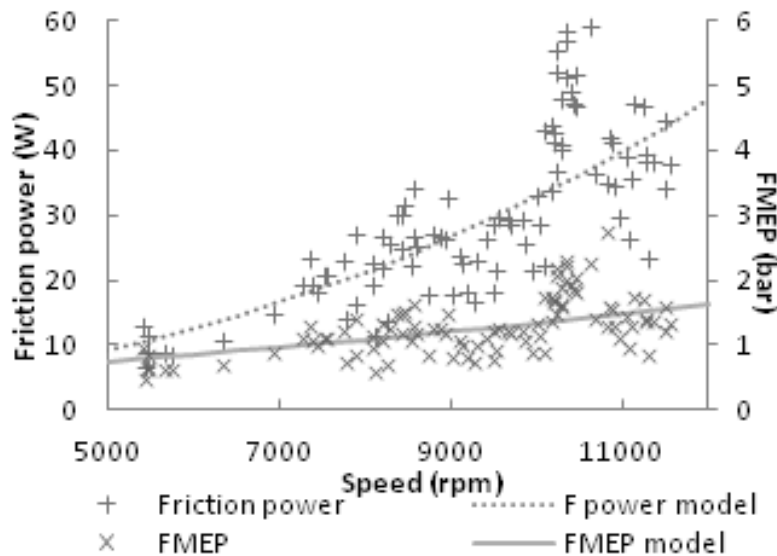

Fig. 3. Friction mean effective pressure (FMEP) and friction power at different engine speeds.

2.4. Scavenging

The scavenging model for a two-stroke engine was used to establish the relation between delivery ratio and charging efficiency. Delivery ratio, the ratio of charge that goes through transfer port during scavenging to a reference mass, describes how much air-fuel mixture is used to scavenge down the cylinder. Charging efficiency, the ratio of the retained fuel air mixture to a reference mass, indicates how well the cylinder is refreshed with new charge after scavenging, In a perfect-mixing scavenging model, the fresh charge mixes with exhaust completely when scavenging. This is not desired because ideally the fresh charge should push the exhaust gases out without mixing. In the perfect-mixing model, the relationship between delivery ratio λ and charging efficiency η_C is [16]

$$\eta_C = 1 - e^{-\lambda}$$

Short circuiting of the air-fuel charge occurs when the inlet mixture travels straight through to the exhaust port, and is an even worse case. A perfect mixing with short circuiting scavenging model was created by adding a short circuiting parameter s to the above perfect mixing model

$$\eta_C = 1 - e^{-(1-s)\lambda}$$

In this model, it was assumed that the perfect mixing portion (1-s) of the fresh charge entered the cylinder and mixes with the gas content inside the cylinder instantly to form a homogeneous mixture, while the remainder of the incoming charge went out of the cylinder directly.

Scavenging was characterized by running the 1.5 cc 2-stroke engine. The mass of the retained air-fuel mixture was inferred from the mass of burned fuel assuming a combustion efficiency of 90%. The experimental data for charging efficiency as a function of delivery ratio is shown in Fig. 4. Retention efficiency is the percentage of supplied fuel air mixture that is retained inside the cylinder after scavenging process and the engine had a retention efficiency of about 45%, which means that more than half the air-fuel mixture was lost during scavenging. The measured charging efficiency of the model engine was worse than a perfect-mixing model because the scavenging system was not optimized to retain more charge and minimize short-circuiting. The experimental data could be reasonably described by the short circuiting model as shown in Fig. 4.
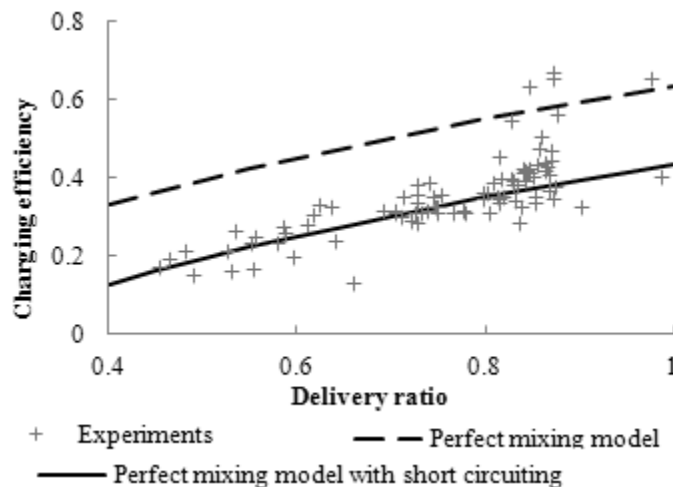

Fig. 4 Simulation and experimental results of model engine scavenging. The data fit a perfect-mixing model that including short circuiting.

Two-stroke engines have more cyclic variation than four-stroke engines because of cycle to cycle variations in scavenging. Slight variations in the gas flow pattern inside the cylinder strongly affect scavenging and thus how much fresh charge is retained in the cylinder for combustion. Also, because the in-cylinder gas composition is not homogeneous, variation of the composition near the glow plug leads to variation in ignition.

Because there are no simple physical models for variation, the experimental data of the model engine were analyzed. Figure 5 shows the frequency distribution of charging efficiency over 181 consecutive cycles at fixed engine speed, load and carburetor setting.
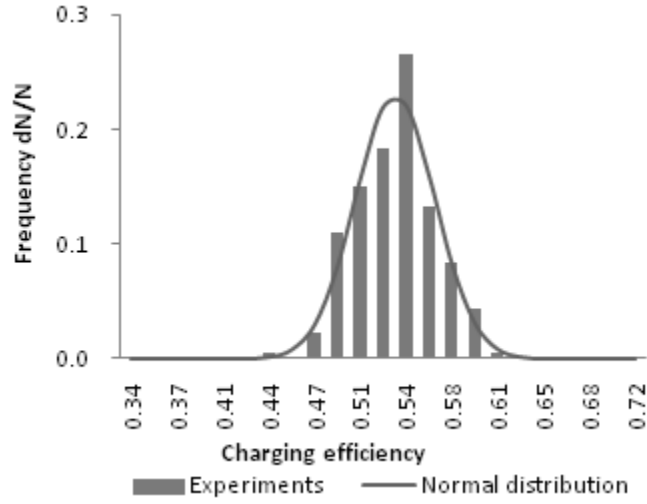

Fig. 6 Distribution of charging efficiencies of 181 cycles

Based on the distribution shown in the figure, the cyclic variation was modeled by a normal distribution of the short circuiting portion parameter s of the scavenging model with a probability function

$$f(s) = \frac{1}{\sqrt{2\pi\sigma^2}} e^{-\frac{(s-\bar{s})^2}{2\sigma^2}}$$

The average short circuiting ratio $\bar{s}$ was determined by the scavenging model while parameter σ was determined by the fitting the probability function to the experimental data of Fig. 6. The result was $\sigma/\bar{s} = 6\%$.

2.5. Piston assembly dynamics

The motion of the free-piston assembly is determined by force balance among the pressure inside the engine cylinder, engine crankcase and compressor cylinder, the friction force, f, and the return spring force, F_{spring}.

$$m dv_{piston}/dt = \left(P_{eng\ cyl} - P_{crankc}\right)A_{eng\ pist} - \left(P_{comp\ cyl} - P_{atm}\right)A_{comp\ pist} - F_{spring} - f$$

For this equation, piston areas and spring constant were measured directly from the components.

3. Engine design

We used the parameterized model to examine the critical factors that influence engine/compressor performance. The free-piston engine is a damped spring-mass system

consisting of the rebound spring and the piston assembly. The combustion accelerates the mass and converts expansion work to kinetic energy of the piston and potential energy of the mechanical and compressed air springs. Friction and discharge of compressed air dissipates energy.

We evaluated the trade-off between leakage and friction to determine the optimum operating speed of the engine (Fig. 7). High engine speed reduces leakage and heat transfer losses (Fig. 2) but increases friction losses (Fig. 3). The retention efficiency indicates how much mixture is retained inside the cylinder without leaking through the cylinder-piston gap. At lower speed more of the cylinder charge is lost due to leakage. At higher speed, mechanical efficiency drops due to friction. From the combined efficiency curve, the engine's best operating range for the engine is between 100 and 150 Hz (Fig. 7). With vibration and noise factors in mind, we chose the target speed to be 100 Hz.
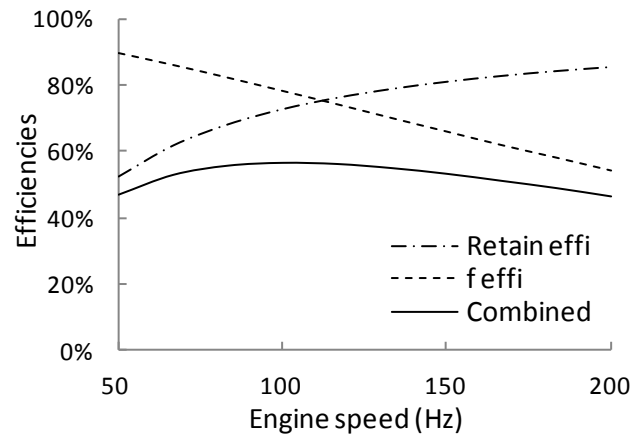

Fig. 7. Predicted in-cylinder charge retention, mechanical and total efficiency as a function of engine speed.

With the operating speed specified, we could determine the engine size because the target output, 20 W of pneumatic power was known. For building the prototype engine, we used the cylinder liner and piston components parts from an R/C engine (Hornet .09, AP Engines) whose 12.5 mm bore and 12 mm stroke were close to the desired values for engine size. We picked a rebound spring with a stiffness of 1350 N/m and set a preload of 25.7 N to provide the necessary energy for engine compression. Spring stiffness and piston assembly moving mass are the main parameters that determine the engine operating speed so we then adjusted the mass of the piston and connecting rod assembly to produce the desired operating frequency. The selected mass was 34.3 grams, which the engine/compressor model predicted would result in an operating frequency of 120 Hz. The prototype shown in Fig. 1 was then constructed based on these selected design parameters.

3. Prototype testing

3.1 Materials and methods

We built and tested a prototype to validate the system model and to determine overall performance. The prototype used the cylinder liner and piston components from an AP Engines .09 R/C engine. The remaining parts were fabricated from aluminum, steel and polymer stock.

The experimental apparatus for testing is shown in Fig. 8. A high bandwidth, high resolution laser triangulation sensor was used to measure piston position (MTI Instrument, model LTC-120-20-SA). A small optical type pressure sensor was used to measure in-cylinder pressure (OPTRAND, model D22255-Q). The compressor output was connected to a 530 mL air tank through an additional check valve to retard leakage through the compressor output valve.
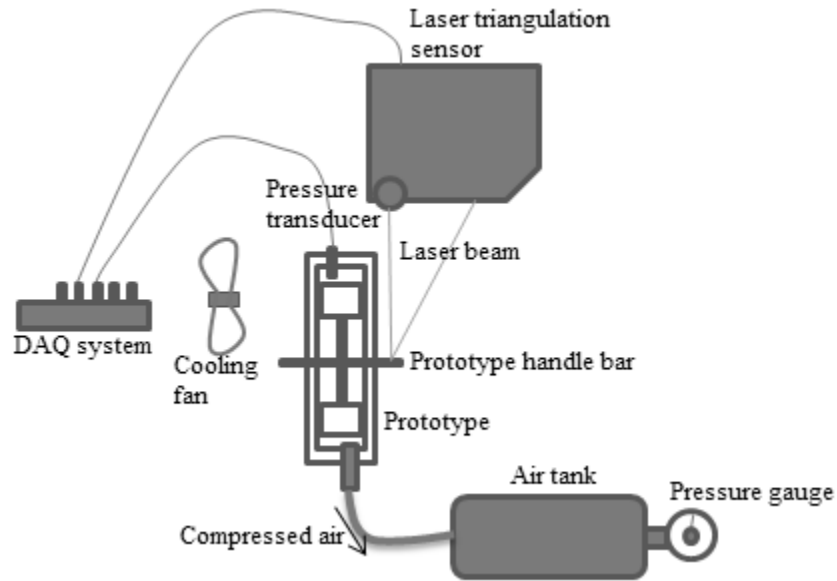

Fig. 8. Prototype experiment test apparatus.

3.2 Overall performance

To start the prototype, the starting handle was pulled by hand to compress the rebound spring. After the piston reached its bottom position with the spring fully compressed, the handle was released to initiate the first cycle. After several manual priming cycles to purge the cylinder and fill it with fresh fuel air mixture, ignition occurred and the engine entered steady state running within a few cycles (Fig. 9). The first two combustion events were weak, reaching peak pressure of about 15 bar, just enough to push the piston past the transfer port open (TO) position at 10.9 mm. In a later cycle, the piston completely passed the TO position and scavenging occurred supplying the engine with a fresh fuel-air charge for the next cycle.
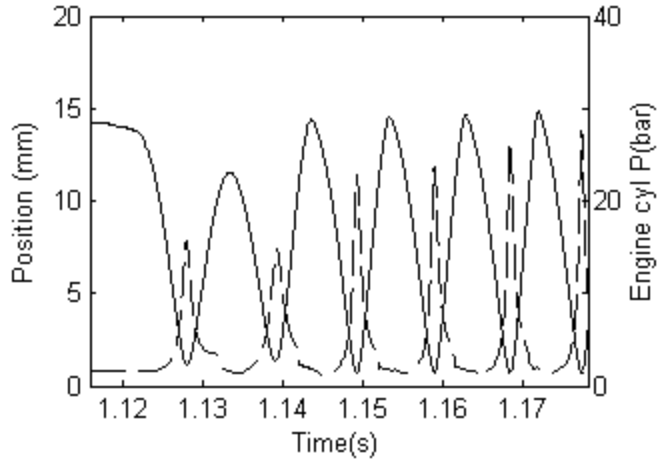
Fig. 9. Startup behavior of the engine/compressor showing cylinder position (solid) and pressure (dashed) for six combustion cycles.

When the engine/compressor charged a reservoir, the output pressure on the compressor gradually increased (Fig. 10). This increased the effective stiffness of the rebound spring, which changed the natural frequency of the engine as predicted by the model. The indicated mean effective pressure (IMEP) of the engine, based on a volume of 1.47 cc (the volume of an equivalent crankshaft engine) was about 3 bar, lower than the typical 4 bar of the equivalent crank shaft engine because of a less effective scavenging process and a lower cycle efficiency, as will be explained later. By calculating the amount of energy stored in the air tank we estimated the output compressed air power be 5 W, lower than the 48 W engine output calculated from the p-V work done on the piston. The losses are due to compressor leakage, friction and compression heating. The device compressed air to 6.5 bar with an overall fuel to cold compressed air efficiency of 0.6%.
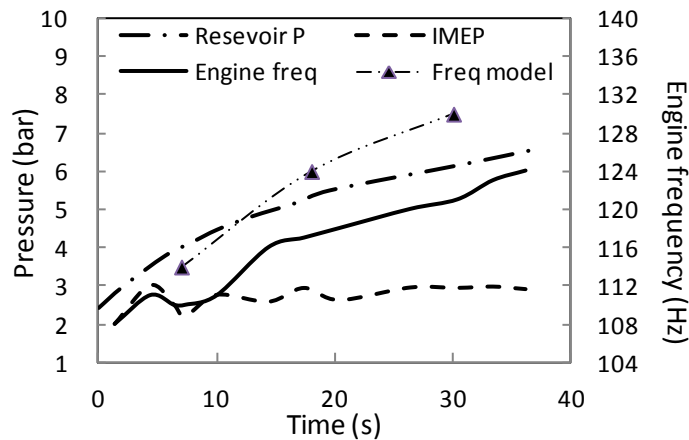

Fig. 10. Engine/compressor charging a 530 mL reservoir.

Unlike a crankshaft engine, the motion of the free-piston engine is dictated by the balance of forces on each side of the piston. The model correctly predicts this motion and demonstrates how it differs from the motion of a crankshaft engine (Fig. 11).
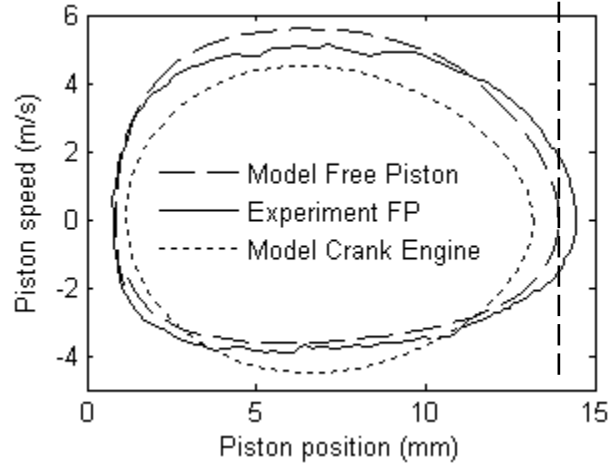

Fig. 11. Position-speed of the piston. Experimental data from a typical cycle of the engine/compressor running at steady state is shown along with the cycle predicted by the model. The third trace is the predicted cycle for an equivalent crankshaft engine. The vertical dashed line marks the position of a rubber limit stop bumper designed to control excessive motion during a strong combustion cycle. As the piston travels beyond (to the right of) the bumper, the kinetic energy of the moving mass is dissipated in the collision. The speed of piston at the collision point indicates how much energy is wasted in the bumper collision.

3.3 Combustion analysis

A combustion analysis was conducted using a heat release analysis method, calculating an energy balance with the combustion chamber as the control volume. The energy balance in the engine cylinder is

$$m_{cv} c_v \frac{dT}{dt} = \dot{Q}_{fuel} + \dot{Q}_{HT} - \dot{W} - \sum \dot{m}_{leak}(h_{cv} - u_{cv})$$

where m, c_v, T, Q, W, h and u are mass, constant volume specific heat, temperature, heat, work, enthalpy and internal energy, cv indicates the control volume, and the terms on the right side are fuel combustion heat change, heat transfer, work output and internal energy loss due to leakage. The temperature at each time step was calculated from measured in cylinder pressure and Annand's heat transfer model [17] was used to calculate heat transfer between the in cylinder charge and the cylinder. The leakage model described above was fit to the experimental data and used model leakage loss. The result of the combustion analysis yielded an estimate of mass fraction burned (MFB) as a function of time during a cycle.

The heat release results for three cycles are shown in Figure 12. Ignition timing was consistent while combustion speed varied. In most cycles combustion was slow, lasting until the exhaust port opened, however some cycles, for example cycle 75 in the figure, had a desirable

fast combustion that finished just past top dead center (TDC). An internal combustion engine achieves its highest possible thermal cycle efficiency if combustion happens instantaneously at top dead center, the characteristic of an ideal Otto cycle. The differences in combustion speed seen in our engine are explained by the cyclic variation of exhaust residue content, mixture composition and mixture motion in the combustion chamber.
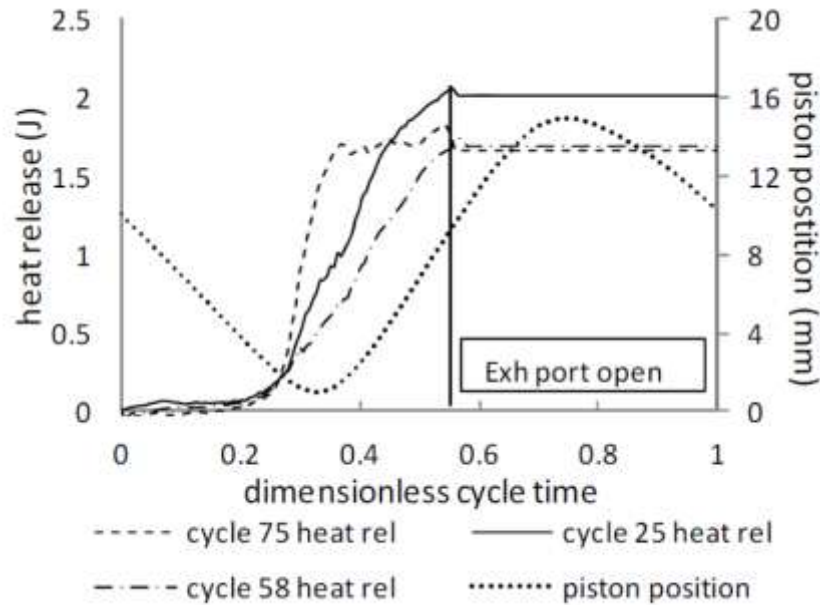

Fig. 12. Heat release for three engine cycles. Cycle 75 had the fastest combustion process, which occurred near TDC. The piston position trace shows the piston approximated sinusoidal motion as predicted by the resonant system model. TDC occurs when the piston is at its minimum position.

Figure 13 shows the pressure-volume data for the same three cycles. Cycle 75 with fast combustion had significant pressure rise before the piston reached TDC. This resulted in a smaller compression ratio as the piston was brought to a stop earlier. Because the entire combustion process was fast and happened entirely near TDC where the pressure is high, rather than lasting throughout the expansion stroke, the faster heat release offset the effects of the lower compression ratio, resulting in a higher cycle thermal efficiency. MFB at TDC is a good indication of how fast and how early the combustion process occurred. For slow cycle 58, MFB was 27% and cycle efficiency was 17% while for fast cycle 75, MFB was 78% and cycle efficiency was 23%.
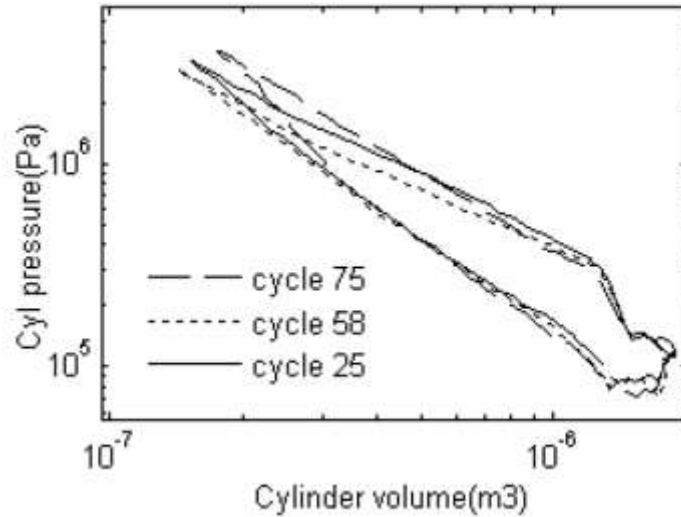
Fig. 13. Pressure-volume traces for the same three cycles as Figure 12. Fast cycle 75 had a significant pressure rise before reaching TDC.

3.4 Self-regulation of compression ratio

We wanted the engine/compressor to be self-regulated without using active control, however, variations in the cycle-to-cycle fuel charge cause variations in the expansion stroke. In a weak cycle, the piston may not travel far enough to completely uncover the exhaust and transfer ports and the scavenging process will be interrupted resulting in engine stall on the next cycle. In a strong cycle, the piston may travel too far and destructively collide against the end stop.

To accommodate this variation, the device was designed to have 2 mm over-stroke, which means the pistons could travel 2 mm further than the nominal bottom dead center (BDC) position of a crankshaft engine. In strong cycles, the pistons will travel further than nominal BDC with the rebound spring and compressor absorbing the additional energy. If the piston travels past the end of the 2 mm over-stroke, a rubber bumper absorbs any extra energy. Fig. 14 diagrams this energy balance for a range of combustion energy release..
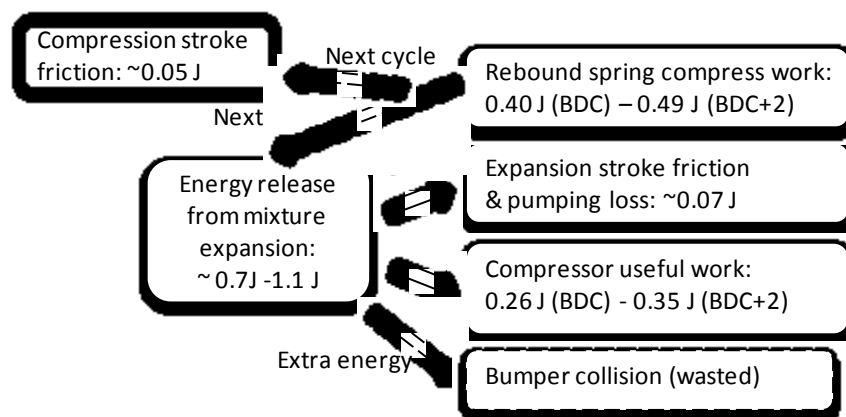

13

Fig. 14. Energy balance for one engine/compressor cycle, running at an output pressure of 4.5 bar.

Using the heat release analysis described in the previous section we calculated MFB at TDC, cycle efficiency and compression ratio for 570 consecutive cycles while the engine was running at steady state with the results shown in Fig. 15. The compression ratio was defined as the cylinder volume when the exhaust ports are just closed by the piston divided by the cylinder volume with the piston at (TDC). This is the effective compression ratio for a two-stroke engine. Because free-piston engines do not have a fixed stroke, their compression ratio changes from cycle to cycle. MFB at TDC indicates how fast and how early combustion occurs.

Figure 15a shows efficiency vs. MFB and confirmed that efficiency increased with combustion speed for the prototype engine, as expected. Figure 15b shows that the device adapted its compression ratio to the variations in combustion process. As in Fig. 13, high MFB meant rapid pressure rise which stopped the piston early resulting in a lower compression ratio. Low MFB meant the mixture was difficult to ignite or slow to burn allowing the piston to travel further upwards resulting in a higher compression ratio. As indicated in Fig. 15b, the compression ratio was as high as 11 for some cycles. This ability to self-regulate is only possible when a free-piston configuration is used.
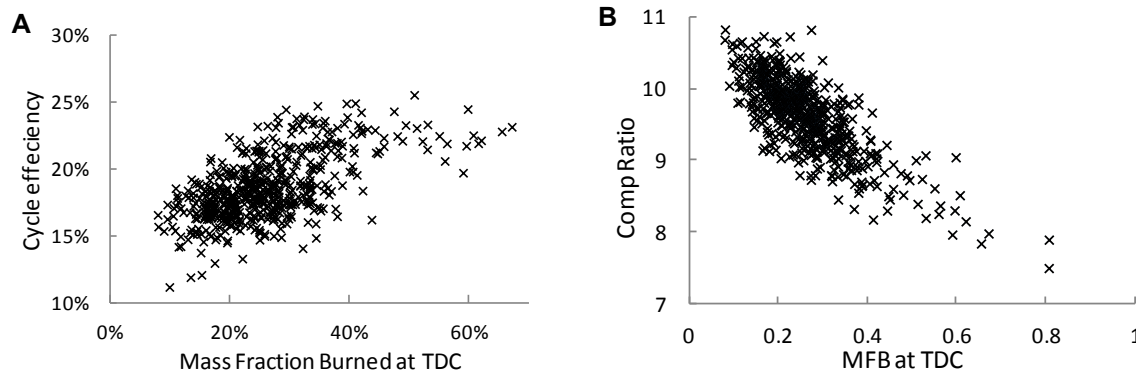

Fig. 15. Calculated cycle properties for experimentally measured 570 consecutive cycles of the engine/compressor. (**A**) Cycle efficiency vs. MFB at TDC. (**B**) Compression ratio vs. MFB at TDC.

3.5 Pressure-volume characteristics

The experimentally measured pressure-volume (p-V) curves (Fig. 16) of the prototype engine/compressor revealed important characteristics that differentiate our engine from a traditional crankshaft engine. As can be seen in 16a, the slope of the expansion line (upper) of the engine/compressor is lower than that of the compression line (lower) indicating that combustion continued throughout the expansion process for the free-piston engine. Also shown in 16a is the measured p-V curve for a comparably sized crankshaft engine. Here the entire combustion occurred near TDC. In the crankshaft engine, after ignition, the piston is effectively held near TDC by the crankshaft and connecting rod allowing time for the combustion to complete, thus the crankshaft engine was close to an ideal, high thermal efficiency Otto cycle

where combustion occurs instantaneously at TDC. With an effective compression ratio of 5.3 and modeling leakage the crankshaft engine's average cycle efficiency was estimated to be 22%. In the free-piston engine/compressor the mixture also ignites around TDC but in this position the rebound spring force is low and there is no reaction force from the load as the compressor side is at the end of its intake stroke. Without a holding force the piston rapidly retreats from TDC outpacing the combustion. This decreases the pressure and temperature in the combustion chamber and results in combustion duration of about 3 ms, compared to 1.4 ms for the crankshaft engine. Even though the free-piston configuration had a higher effective compression ratio of about 10, its average cycle efficiency was estimated to be 18%.

Figure 16b compares the measured p-V curve to the p-V curve predicted by the model. The deviation between the measured and modeled glow plug curves that occurs in the compression process (lower curve) indicates that the real engine had a higher polytrophic index during the compression stroke than that predicted by the model. This is because the model does not estimate exhaust residue content in the cylinder, cylinder wall temperature or the lubrication oil present in the piston cylinder gap which helps to seal the gap from leakage.

The efficiency of the free-piston engine-compressor can be improved with a faster combustion process. Our prototype used glow plug ignition and associated flame propagation [18–20], however, with true HCCI, the mixture ignites nearly simultaneously everywhere in the combustion chamber [9]. For example, Aichlmayer realized true HCCI in single-shot combustion in a 3 mm cylinder and showed with high-speed video that HCCI combustion took less than 60 μs [12]. Figure 16b shows the predicted p-V curve for the same free-piston engine/compressor where combustion is modeled as true HCCI rather than glow plug. The HCCI model predicts that the p-V curve will have a steep rise of pressure due to fast heat release and that the cycle efficiency will be 41% compared to 25% for glow plug ignition. Part of the efficiency gain is because of the larger compression ratio (12.3 for HCCI compared to 9.0 for glow plug ignition), while the rest is due to the faster heat release.
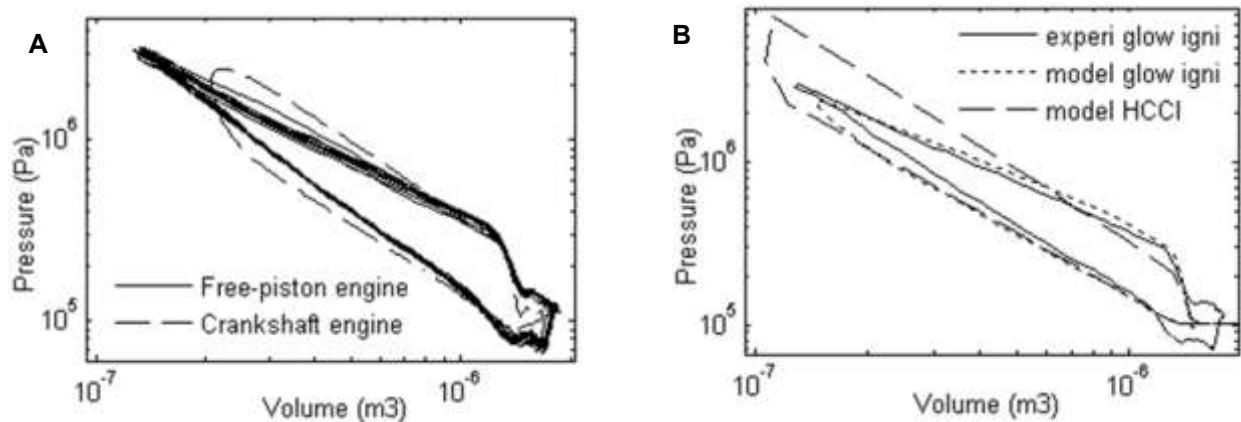

Fig. 16. Pressure-volume (log-log) curves for an operating engine. (**A**) Experimentally measured data for 12 cycles of the free-piston engine and one cycle of a crankshaft engine matched in size. (**B**) Model validation. One experimentally measured cycle from the glow plug engine/compressor compared to what the model predicts, along with the model prediction for one cycle of the equivalent HCCI engine.

4. Discussion

Our free-piston engine/compressor demonstrates that a small-scale internal combustion air compressor is technically feasible and can attain reasonable efficiencies. Further, the prototype engine validated the mathematical model, which means the model can be used to optimize the device design. The prototype produced about 5 W of pneumatic output at up to 8.2 bar.

For this engine, in-cylinder mixture leakage was severe as the leakage model suggested that at least one third of the in-cylinder charge escaped through the piston cylinder gap during compression, combustion and expansion, resulting in significant enthalpy loss from the combustion chamber. Thus, one of the best ways to improve the device efficiency is to design a better lubrication and sealing system to contain the leakage.

A second important way to improve the efficiency is to switch from glow plug ignition to true HCCI. While the model over-predicted the cycle efficiency measured in the actual engine, the model does predict that cycle efficiency with HCCI will be significantly higher than with glow plug ignition.

In addition to improving the overall efficiency, before the free-piston engine/compressor can be used in a practical application, three important technical issues must be addressed. First, a practical starting method must be devised. Second, a reliable fuel delivery system must be designed. Third, noise and vibration must be reduced. We believe these issues are not insurmountable and are optimistic that someday the engine/compressor can be used as a practical portable power supply.

References

1. Mikalsen R, Roskilly AP. A review of free-piston engine history and applications. *Applied Thermal Engineering.* 2007 Oct;27(14–15):2339–2352.

2. Pescaba EP. Motor-Compressor Apparatus. 1928 Jan 31;

3. Toutant WT. The Worthington-Junkers Free Piston Air Compressor. *Journal of the American Society for Naval Engineers.* 1952;64(3):583–594.

4. Braun AT, Schweitzer PH. The Braun Linear Engine. SAE International; 1973.

5. Riofrio JA, Barth EJ. A Free Piston Compressor as a Pneumatic Mobile Robot Power Supply: Design, Characterization and Experimental Operation. *Int J Fluid Power.* 2007;8(1):17–28.

6. Annen KD, Stickler DB, Woodroffe J. Miniature Internal Combustion Engine-Generator for High Energy Density Portable Power. Defense Technical Information Center; 2008.

7. Huber R. Present State and Future Outlook of the Free-Piston Engine. *Trans ASME.* 1958;80(8):1779–1790.

8. Achten PAJ, Van Den Oever JPJ, Potma J, Vael GEM. Horsepower with Brains: The Design of the CHIRON Free Piston Engine. SAE International; 2000.

9. Onishi S, Jo SH. Active Thermo-Atmosphere Combustion (ATAC) ---A New Combustion Process for Internal Combustion Engines. SAE International; 1979.

10. Aichlmayr HT, Kittelson DB, Zachariah MR. Miniature free-piston homogeneous charge compression ignition engine-compressor concept—Part I: performance estimation and design considerations unique to small dimensions. *Chem Eng Sci.* 2002 Oct;57(19):4161–4171.

11. Aichlmayr HT, Kittelson DB, Zachariah MR. Miniature free-piston homogeneous charge compression ignition engine-compressor concept—Part II: modeling HCCI combustion in small scales with detailed homogeneous gas phase chemical kinetics. *Chem Eng Sci.* 2002 Oct;57(19):4173–4186.

12. Aichlmayr HT, Kittelson DB, Zachariah MR. Micro-HCCI combustion: experimental characterization and development of a detailed chemical kinetic model with coupled piston motion. *Combustion and Flame.* 2003 Nov;135(3):227–248.

13. Tian L, Kittelson D, Durfee W. Experimental Tests and Simulations of A 1.5 cc Miniature Glow-Ignition Two-Stroke Engine. SAE International; 2010.

14. Sher I, Levinzon-Sher D, Sher E. Miniaturization limitations of HCCI internal combustion engines. *Applied Thermal Engineering.* 2009 Feb;29(2–3):400–411.

15. Heywood JB, Sher E, Engineers S of A. The Two-Stroke Cycle Engine: Its Development, Operation, and Design. Taylor & Francis; 1999.

16. Blair GP. Design and Simulation of Two-Stroke Engines. Society of Automotive Engineers; 1996.

17. Annand WJD. Heat Transfer in the Cylinders of Reciprocating Internal Combustion Engines. *Proc Inst Mech Eng.* 1963 Jun 1;177(1):973–996.

18. Ogawa T, Kawaguchi Y. Performance Testing of 5cc Glow-Ignition Four-Stroke Engine [Internet]. In: ASME/JSME 2007 Thermal Engineering Heat Transfer Summer Conference. ASME; 2007 [cited 2012 Jul 5]. p. 807–814.Available from: http://link.aip.org/link/ASMECP/v2007/i42762/p807/s1&Agg=doi

19. Raine RR, Thorwarth H. Performance and Combustion Characteristics of a Glow-Ignition Two-Stroke Engine. SAE International; 2004.

20. Ma H, Kar K, Stone R, Raine R, Thorwarth H. Analysis of Combustion in a Small Homogeneous Charge Compression Assisted Ignition Engine. *Int J Engine Res.* 2006 Jun 1;7(3):237–253.